Ott, I., Duethmann, D., Liebert, J., Berg, P., Feldmann, H., Ihringer, J., Kunstmann, H., Merz, B., Schaedler, G., Wagner, S. (2013): High-Resolution Climate Change Impact Analysis on Medium-Sized River Catchments in Germany: An Ensemble Assessment. - *Journal of Hydrometeorology*, *14*, 1175-1193

DOI: 10.1175/JHM-D-12-091.1

# High-Resolution Climate Change Impact Analysis on Medium-Sized River Catchments in Germany: An Ensemble Assessment

IRENA OTT,*,+ DORIS DUETHMANN,# JOACHIM LIEBERT,@ PETER BERG,& HENDRIK FELDMANN,**
JUERGEN IHRINGER,@ HARALD KUNSTMANN,++ BRUNO MERZ,#
GERD SCHAEDLER,** AND SVEN WAGNER*

* *Atmospheric Environmental Research, Institute for Meteorology and Climate Research (IMK-IFU), Karlsruhe Institute of Technology, Garmisch-Partenkirchen, Germany*
# *Section 5.4–Hydrology, GFZ German Research Centre for Geosciences, Potsdam, Germany*
@ *Hydrology, Institute for Water Resources and River Basin Management (IWG), Karlsruhe Institute of Technology, Karlsruhe, Germany*
& *Rossby Centre, Swedish Meteorological and Hydrological Institute, Norrköping, Sweden*
** *Troposphere Research, Institute for Meteorology and Climate Research (IMK-TRO), Karlsruhe Institute of Technology, Eggenstein-Leopoldshafen, Germany*
++ *Atmospheric Environmental Research, Institute for Meteorology and Climate Research (IMK-IFU), Karlsruhe Institute of Technology, Garmisch-Partenkirchen, and Department of Geography, University of Augsburg, Augsburg, Germany*

(Manuscript received 21 June 2012, in final form 21 February 2013)

ABSTRACT

The impact of climate change on three small- to medium-sized river catchments (Ammer, Mulde, and Ruhr) in Germany is investigated for the near future (2021–50) following the Intergovernmental Panel on Climate Change (IPCC) Special Report on Emissions Scenarios (SRES) A1B scenario. A 10-member ensemble of hydrological model (HM) simulations, based on two high-resolution regional climate models (RCMs) driven by two global climate models (GCMs), with three realizations of ECHAM5 (E5) and one realization of the Canadian Centre for Climate Modelling and Analysis version 3 (CCCma3; C3) is established. All GCM simulations are downscaled by the RCM Community Land Model (CLM), and one realization of E5 is downscaled also with the RCM Weather Research and Forecasting Model (WRF). This concerted 7-km, high-resolution RCM ensemble provides a sound basis for runoff simulations of small catchments and is currently unique for Germany. The hydrology for each catchment is simulated in an overlapping scheme, with two of the three HMs used in the project. The resulting ensemble hence contains for each chain link (GCM–realization–RCM–HM) at least two members and allows the investigation of qualitative and limited quantitative indications of the existence and uncertainty range of the change signal. The ensemble spread in the climate change signal is large and varies with catchment and season, and the results show that most of the uncertainty of the change signal arises from the natural variability in winter and from the RCMs in summer.

## 1. Introduction

The Intergovernmental Panel on Climate Change (IPCC) Fourth Assessment Report (AR4; Christensen et al. 2007) summarizes possible effects of global climate change for Europe. While a future warming is projected for all of Europe, mean precipitation is projected to decrease in the south and increase in the north. So, projections of future precipitation in central Europe are fraught with high uncertainties. Knowledge of the impact of climate change on hydrological systems and especially flood discharges is important for the adaptation of existing and planning for future flood management. Whereas larger river systems in Europe and Germany have been widely studied (e.g., Kleinn et al. 2005; Dankers and Feyen 2008; Hurkmans et al. 2010), there is

+ Current affiliation: Department of Geography, University of Augsburg, Augsburg, Germany.

*Corresponding author address:* Irena Ott, University of Augsburg, Department of Geography, Universitaetsstrasse 10, 86135 Augsburg, Germany.
E-mail: irena.ott@geo.uni-augsburg.de

DOI: 10.1175/JHM-D-12-091.1

still a lack of information on climate change impacts on smaller rivers. Smaller catchments require higher spatial resolution of the driving atmospheric models, and with decreasing spatial extent the uncertainty of any climate change signal is likely to increase.

The uncertainties of climate projections arise from each step of the model chain from the global, via the regional, climate modeling to the hydrological modeling. On the global scale, uncertainty arises from the choice of the global climate model (GCM), the internal variability of the climate system, and the choice of the future emission pathway. The variability of the greenhouse gas emissions is not a main factor of uncertainty for the near future (e.g., Andréasson et al. 2004; Graham et al. 2007) and is therefore neglected here. Thus, only the IPCC Special Report on Emissions Scenarios (SRES) A1B scenario was used in this project to be able to focus on other sources of uncertainty, for example, natural variability. Also on the regional climate model (RCM) and hydrological model (HM) level, the models differ in their representation of the processes and the regional characteristics. A full coverage of the uncertainties at each individual model chain level has been performed in other studies [e.g., the Coupled Model Intercomparison Project (CMIP) (Meehl et al. 2000) and Ensemble-Based Predictions of Climate Changes and their Impacts (ENSEMBLES) (Hewitt and Griggs 2004)]. Although it would be desirable to fill the matrix of possible outcomes on all levels simultaneously, this is beyond the focus of the study and has not even been covered by large international programs.

This study aims at illustrating the contribution of the different uncertainty sources to the overall uncertainty by using at least two examples of each level of the model chain. On the global scale this is covered by using two different GCMs and three realizations for one of the GCMs. The regional climate is covered by two different RCMs, and the hydrological modeling is performed with three HMs applied to two catchments each. Although the ensemble might be too small for quantitative statistical inference, qualitative insight into the sources of uncertainty can be gained from this small but systematic ensemble.

Our high-resolution RCM ensemble is currently unique for Germany and presents a concerted modeling effort both for RCM simulations and hydrological modeling, resulting in a consistent model chain for the hydrological impact analysis of climate change in Germany. The model chain was implemented for the Ammer, Mulde, and Ruhr catchments—chosen to represent different flood regimes in Germany (Beurton and Thieken 2009).

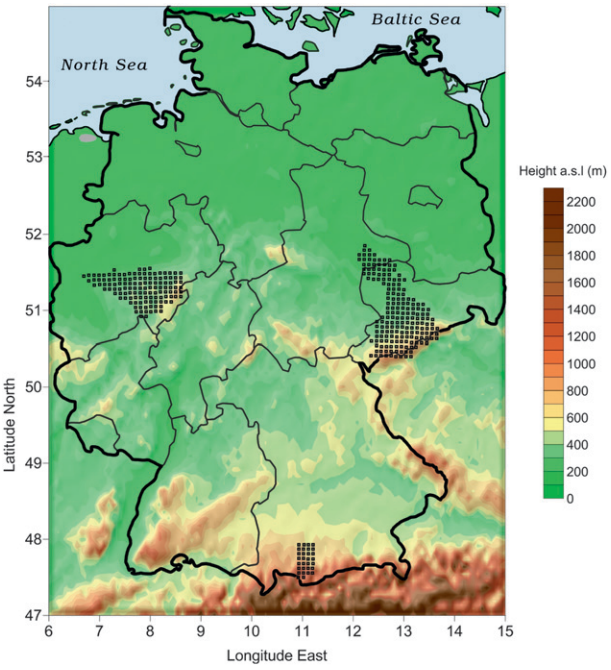


FIG. 1. Location of the three investigated catchments (black stipple pattern) in Germany. Flow directions: Ammer (south) and Mulde (east) from south to north, Ruhr (west) from east to west. The black lines indicate the borders of Germany and the states within Germany.

The three study areas are described in section 2, and the analysis of the climate data input is presented in section 3. Section 4 contains the description of the applied HMs and their calibration/validation results; section 5 presents the climate change impact on hydrology and an analysis of the uncertainties within the model chain. The article closes with discussion and conclusions in section 6.

## 2. Study area

For this study, three small- to medium-sized river catchments in Germany were chosen. They represent different flood regimes in Germany as described by Beurton and Thieken (2009): dominant winter floods in the Ruhr catchment as typical for central and western Germany; winter, but also spring and summer, floods in the Mulde as typical for north and east Germany; and summer floods in the Ammer catchment as typical for the alpine south. The locations of the three catchments are shown in Fig. 1, and a summary of the most important hydrological characteristics of the three catchments is given in Table 1.

The smallest catchment is the alpine Ammer (about 710 $km^2$), which is part of the Danubian river system. It is characterized by a large elevation gradient

TABLE 1. Characteristics of the three catchments investigated and mean discharges and runoff: mean monthly discharge (MQ), mean runoff rate (Mq), mean maximum monthly discharge (MHQ), and mean maximum runoff rate (Mhq). The ranges of annual precipitation sums represent the variability within the catchment area.

| | Ammer | Mulde | Ruhr |
|---|---|---|---|
| Size ($km^2$) | 710 | 6171 | 4485 |
| River system | Danube | Elbe | Rhine |
| Elevation (m) | 533–2185 | 50–1244 | 20–850 |
| Typical land use | 49% grassland | 52% cropland | 52% forest |
| | 41% forest | 30% forest | 32% grassland |
| | 2.4% settled | 7% settled | 8.7% settled |
| Annual mean temperature (°C) | 7 | 8.4 | 9 |
| Annual precipitation sum ($mm\,yr^{-1}$) | 1000–2000 | 600–1000 | 800–1400 |
| Annual mean discharge at downstream gauges | | | |
| MQ ($m^3\,s^{-1}$) | 15 | 64 | 68 |
| Mq [$L\,(s\,km^2)^{-1}$] | 33 | 15 | 23 |
| MHQ ($m^3\,s^{-1}$) | 164 | 481 | 541 |
| Mhq [$L\,(s\,km^2)^{-1}$] | 492 | 154 | 241 |
| Degree of regulation | low | middle | high |

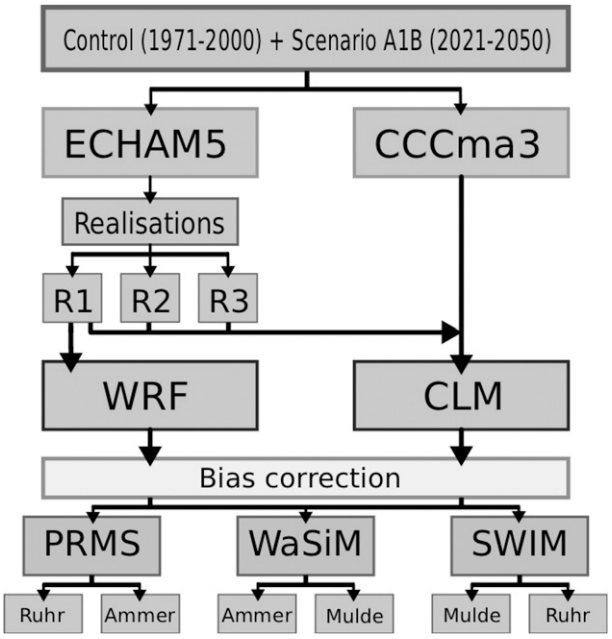


FIG. 2. Schematic flow chart of the ensemble strategy.

from Mount Kreuzspitze at 2185 m to the outlet Lake Ammersee (533 m). The average precipitation amount is 1300 $mm\,yr^{-1}$, and in the southern alpine part values up to 2000 mm occur. Land cover is mainly grassland and forest (mostly coniferous forest), with an increasing percentage of forest in the southern part of the drainage basin. Higher altitudes are snow covered for approximately 130 $days\,yr^{-1}$. The flow regime of the Ammer is influenced by two factors: snowmelt in spring and a precipitation maximum in summer. As a result, maximum monthly discharge values occur in May in alpine subcatchments and in June and July for the downstream subcatchments (Marx et al. 2006; Kunstmann et al. 2005).

The largest analyzed catchment is the Mulde River with about 6171 $km^2$, located in eastern Germany. It drains the northern part of the Ore Mountains and is a tributary of the Elbe. The southern part of the drainage basin is mountainous with an elevation maximum of 1244 m, and in the northern part elevations decrease to 50 m. Forest areas are concentrated in the mountainous part of the catchment, and in the lowlands the dominant land use is agriculture. There is a north–south gradient of mean annual precipitation with values of around 600 mm in the lowlands to more than 1000 mm in the Ore Mountains, where precipitation amounts additionally increase from east to west. In comparison to the other two catchments, the Mulde is the driest investigated area. The mean monthly discharge regime is characterized by high flows in March/April caused by rain and snowmelt and minimum flows during the summer months. Monthly maximum flows show peaks in winter and spring but can also occur during low flow conditions in summer.

The Ruhr—the second-largest catchment with 4485 $km^2$—is situated in western Germany and is a right tributary (east side) of the Rhine. The headwaters of the Ruhr are located in the northwest of the Rothaar Mountains. The maximum elevation in the catchment is 850 m. The Ruhr basin is situated in a low mountain range, and wide parts are forest. Extensive urban areas are located in the lower part of the catchment. The monthly discharge regime at the Ruhr shows a typical seasonal cycle. High flows in December to March are caused by intensive rainfalls during the winter period. During the summer months, distinct low flow conditions dominate. Floods are often initiated by snowmelt in the early spring. The Ruhr is highly regulated by abstractions and water reservoirs. Since no scenarios for future abstractions were available and to allow for a better comparability between different HMs, regulation was not considered in this study as a first approximation.

The analysis shown here is based on the downstream gauges of each catchment: Weilheim for the Ammer, Bad Düben for the Mulde, and Wetter for the Ruhr.

## 3. Climate data input

Figure 2 shows the model chain (flow diagram) of this study. For each catchment, an ensemble of 10 members

TABLE 2. Naming conventions for the applied model chain members.

| Model | Name | Abbreviation |
|---|---|---|
| GCMs | ECHAM5 | E5 |
| | CCCma3 | C3 |
| Realizations | 1,2,3 | R1, R2, R3 |
| RCMs | CLM | CLM |
| | WRF | WRF |
| HMs | PRMS | PRMS |
| | SWIM | SWIM |
| | WaSiM-ETH | WaSiM |
| In combination: | | |
| | ECHAM5 (1. realization) + WRF | WRF-E5R1 |
| | ECHAM5 (1. realization) + CLM | CLM-E5R1 |
| | ECHAM5 (2. realization) + CLM | CLM-E5R2 |
| | ECHAM5 (3. realization) + CLM | CLM-E5R3 |
| | CCCma3 + CLM | CLM-C3 |

is available with respect to the two GCMs, ECHAM5 (Roeckner et al. 2003) and Climate Modelling and Analysis version 3 (CCCma3; Scinocca et al. 2008), with three realizations for ECHAM5; the two RCMs, Community Land Model (CLM; Doms and Schättler 2002) and Weather Research and Forecasting Model (WRF; Skamarock et al. 2008); and the three HMs [Precipitation Runoff Modeling System (PRMS), Soil and Water Integrated Model (SWIM), and Water Balance Simulation Model–Eidgenössische Technische Hochschule (WaSiM-ETH); see section 4], each simulating two of the investigated catchments. For an overview of the different models and the abbreviations used, see Table 2. For the control period the years 1971–2000 are chosen; the scenario period includes the 30 years from 2021 to 2050. GCM simulations were provided by the IPCC AR4 ensemble of simulations, and the RCM and HM simulations were performed within the Center for Disaster Management and Risk Reduction Technology (CEDIM) project ''Flood Hazards in a Changing Climate.''

No general rules can be given for the ensemble size required for reliable results of climate change impact studies; it depends on region, season, projection period, quantity, and the statistics (mean, extremes) considered. Some indications are given in Deser et al. (2012). They found that only one realization is needed to detect a significant warming trend in the 2050s compared to the 2010s. But then, approximately 3–6 ensemble members were necessary to find a significant trend of precipitation for tropical and high latitudes, and at least 15 members for the middle latitudes. Reifen and Toumi (2009) found that the ensemble error decreases quickly when the ensemble has more than about 10 members. Feldmann et al. (2013) compared the near-future climate change signal for heavy precipitation obtained from a 17-member ensemble with the results of a larger ensemble and found that the essential information was already contained in the small ensemble. The restricted number of suitable GCMs and the computational demands of the simulations inhibited a larger ensemble in our study. However, this is one of the largest currently available concerted RCM-based ensembles at such a high resolution for Germany.

The global numerical models include representations of the physical processes of the atmosphere, cryosphere, oceans, and land surface. The model simulations follow a procedure of an initial spinup of the full system over several thousand years, until a quasi-stable equilibrium between the ocean and atmosphere is reached. From these simulations several initialization times for the scenario simulations are selected to account for the internal variability of the climate system. Therefore, the three realizations of ECHAM5 follow the same climate forcing, but the different initial conditions allow for the development of unique internal variabilities.

Owing to high computational demands, the GCMs use horizontal resolutions of several hundred kilometers, which is too coarse to drive a high-resolution hydrological model. A dynamical downscaling procedure using regional climate models is therefore applied. The RCMs run offline with boundary fields from GCMs, which is called one-way nesting. To bridge the resolution gap, with a factor of ~30 between the needs of the hydrological models and the grid spacing of the GCMs, a double nesting procedure is used. First, the RCM downscales the GCM data to the coarse nest resolution of ~50 km for all of Europe. In a second step, the RCM is nested within the first nest and downscales the model fields further to a 7-km resolution for all of Germany and its near surroundings (Berg et al. 2013; Wagner et al. 2013). The high spatial resolution provides clear added value to both spatial patterns and the intensity distribution of precipitation, in comparison to coarser models (Berg et al. 2013). The need of high-resolution RCM data (<10 km) for good performance of precipitation and temperature within small investigation areas was shown, for example, by Smiatek et al. (2009).

Both GCMs and RCMs produce biases in their simulations, which may impair their applicability for hydrological modeling (Wilby et al. 2000). A wet bias in annual precipitation could, for example, force the hydrological model into a constantly wet regime, which would have a large influence on the simulated flood characteristics. Hence, the Bias Correction Histogram Equalization - Linear (BCHE-L) bias correction method

TABLE 3. Mean meteorological forcing data (1971–2000) for the three catchments investigated during the winter half-year (WH) and summer half-year (SH).

| | Precipitation (mm month$^{-1}$) | | | Temperature (°C) | | | RH (%) | | | SW radiation (W m$^{-2}$) | | |
|---|---|---|---|---|---|---|---|---|---|---|---|---|
| | Annual | WH | SH | Annual | WH | SH | Annual | WH | SH | Annual | WH | SH |
| | | | | | | Ammer | | | | | | |
| DWD/PIK | **104** | **77** | **132** | **7** | **1** | **13** | **80** | **82** | **78** | **128** | **82** | **173** |
| REGNIE | **120** | **91** | **149** | NA | NA | NA | NA | NA | NA | NA | NA | NA |
| RCMs mean | **122** | **92** | **151** | **7** | **1** | **12** | **81** | **82** | **79** | **111** | **77** | **145** |
| range from | 119 | 89 | 148 | 6 | 0 | 11 | 69 | 75 | 63 | 101 | 72 | 127 |
| to | 125 | 95 | 154 | 7 | 1 | 12 | 84 | 85 | 84 | 145 | 90 | 200 |
| | | | | | | Mulde | | | | | | |
| DWD/PIK | **59** | **52** | **66** | **8** | **3** | **14** | **78** | **82** | **75** | **116** | **66** | **165** |
| REGNIE | **62** | **55** | **69** | NA | NA | NA | NA | NA | NA | NA | NA | NA |
| RCMs mean | **64** | **55** | **72** | **8** | **3** | **14** | **84** | **87** | **82** | **99** | **64** | **133** |
| range from | 63 | 55 | 71 | 8 | 2 | 14 | 73 | 82 | 64 | 91 | 61 | 120 |
| to | 64 | 57 | 73 | 8 | 3 | 14 | 87 | 88 | 86 | 124 | 71 | 177 |
| | | | | | | Ruhr | | | | | | |
| DWD/PIK | **90** | **94** | **86** | **9** | **4** | **14** | **79** | **82** | **77** | **111** | **64** | **158** |
| REGNIE | **91** | **95** | **86** | NA | NA | NA | NA | NA | NA | NA | NA | NA |
| RCMs mean | **93** | **99** | **88** | **8** | **3** | **13** | **87** | **89** | **85** | **90** | **56** | **124** |
| range from | 92 | 97 | 87 | 8 | 3 | 13 | 78 | 85 | 71 | 82 | 54 | 110 |
| to | 96 | 103 | 89 | 9 | 3 | 14 | 90 | 91 | 89 | 113 | 63 | 163 |

was applied to the temperature and precipitation results of the fine-nest RCM data for each of the three catchments (Berg et al. 2012). BCHE-L takes into account the complete distribution of precipitation and temperature values, separately, and calculates a transfer function that maps the model distribution onto that observed. The transfer function is well approximated by a linear fit, which means that changes in the mean and variance are corrected. Monthly correction factors were calculated for the period 1971–2000 for each GCM-RCM simulation, using observational data from Regionalisierung von Niederschlagshöhen [REGNIE; German Meteorological Service (DWD)] and the ENSEMBLES Observational Gridded Dataset (E-OBS) (Haylock et al. 2008) for precipitation and temperature, respectively. Both datasets were interpolated to the RCM grids before calculations were carried out. For WRF-E5R1 and CLM-C3, the corrections were applied directly, but for the three ECHAM5 realizations downscaled with CLM (CLM-E5R1-3) a different approach was used. Although the three downscaled realizations have slightly different bias, this is not because of differences in the ''true'' RCM and GCM biases, but a result of natural variability. If individual corrections were carried out for each CLM-E5 realization, the natural variability in the control period would be removed. To retain this variability, an average of the three sets of correction factors was calculated and applied to each of the CLM-E5 simulations. In the following sections, the observed and simulated meteorological data (for precipitation and temperature bias-corrected values) as well as the future projections are discussed.

### *a. Meteorological forcing data for the three catchments from 1971 to 2000*

Table 3 gives an overview of the meteorological forcing data for the three investigated catchments. Shown are observational datasets [DWD/Potsdam Institute for Climate Impact Research (PIK) contains quality controlled and, if necessary, amended weather data from climate stations of the DWD (Österle et al. 2006) and REGNIE data] as well as the range of the forcing RCM data ensemble within each catchment for annual, winter, and summer precipitation, temperature, relative humidity, and shortwave downward radiation.

For precipitation, the REGNIE dataset in the Ammer catchment has considerably higher values than the DWD/PIK data. The average difference for the catchment amounts to almost 200 mm yr$^{-1}$. For the alpine regions in the south, the differences rise up to 330 mm yr$^{-1}$. Possible reasons for differences between two datasets based on observations are the number of stations considered and their topographical location as well as the applied interpolation method. Also, the REGNIE method (described in Berg et al. 2012) can impact the amounts. That different observational datasets can have large discrepancies was also found by Lorenz and Kunstmann (2012). As RCM precipitation results are

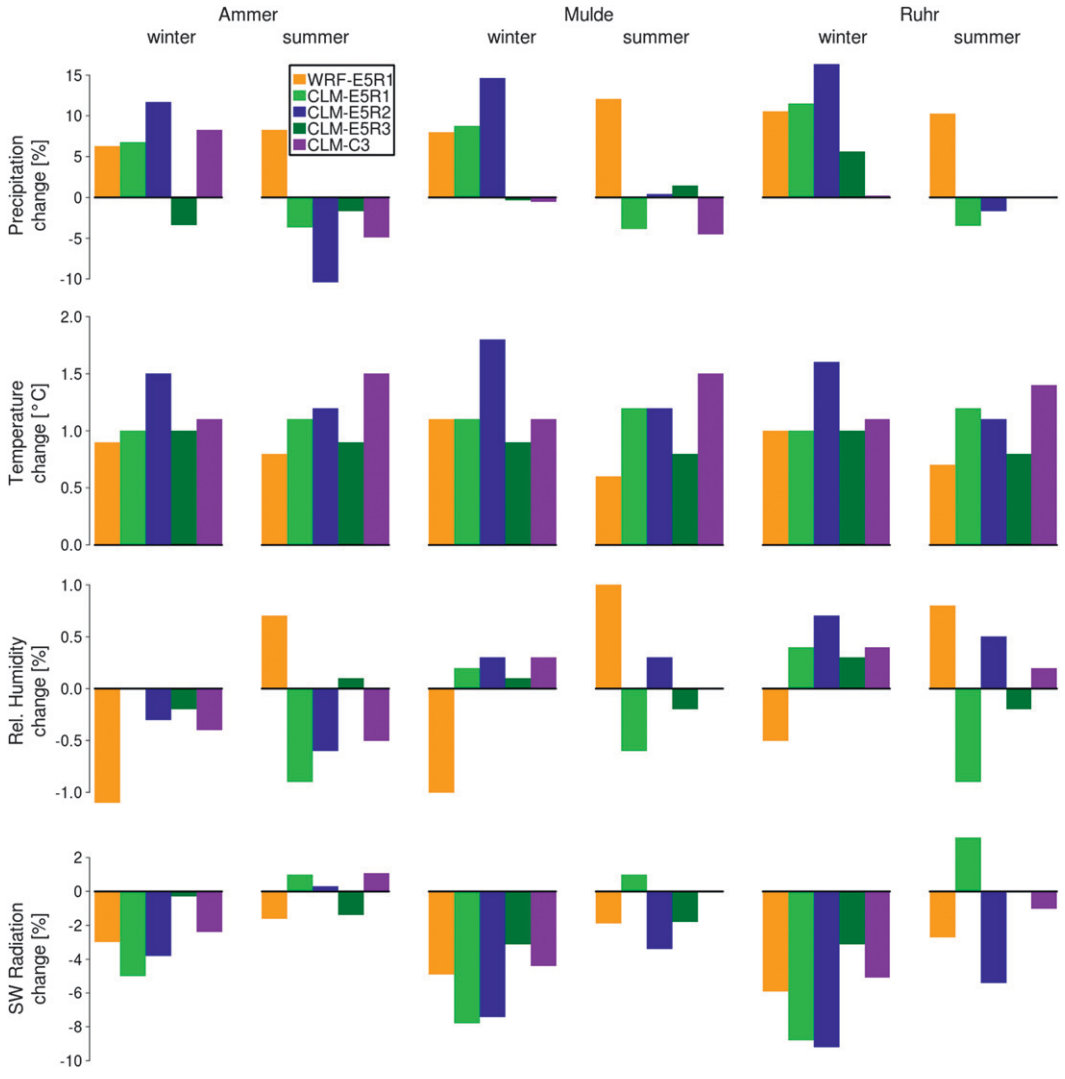


FIG. 3. Projected RCM future changes (2021–50 to 1971–2000) for precipitation, temperature, relative humidity (RH), and shortwave (SW) downward radiation.

bias corrected to the REGNIE data, the resulting RCM precipitation sums fit better to the REGNIE than to DWD/PIK data. For the other two catchments, there are no distinct differences between the observed precipitation datasets. After bias correction, the RCMs are able to describe the seasonal cycle of precipitation well, and the remaining spread between the models after bias correction is mainly due to the natural variability as sampled by the CLM-E5R1-3 simulations.

The bias correction for temperature performs well in all three catchments. Relative humidity, which is not corrected, differs significantly. In the Mulde and Ammer catchments, the RCM WRF underestimates mean annual humidity by up to −14%. The underestimation is more pronounced in summer than in winter. Furthermore, differences between summer and winter half-years are overestimated. In contrast, all Community Land Model (CLM) results overestimate humidity, which is most pronounced in summer at Mulde and Ruhr by up to +15%. The summer − winter differences are smaller than for WRF.

The mean annually accumulated shortwave radiation is underestimated by all single CLM simulations primarily in summer by at least −22%. WRF simulates the solar radiation at the Ruhr catchment well, but for Ammer and Mulde overestimations up to +15% occur, most pronounced in summer.

### *b. Projected future change of the meteorological forcing data*

Figure 3 shows the projected change of the meteorological variables for the scenario period 2021–50 for

TABLE 4. Meteorological input variables for the hydrological models and their applied spatial and temporal resolutions in the Ammer (A), Mulde (M), and Ruhr (R). Shown are subcatchments (SC) and hydrological response units (HRU).

| | | PRMS | SWIM | WaSiM |
|---|---|---|---|---|
| Precipitation | Sum | x | x | x |
| Temperature | Min. | x | x | |
| | Max. | x | x | |
| | Mean | x | x | x |
| RH | Mean | | x | x |
| | Value at 1400 LT | x | | |
| Solar radiation | Sum | | x | x |
| Wind speed | Mean | | | x |
| Temporal resolution | | daily (R,A) | daily (M,R) | daily (M) and hourly (A) |
| Spatial resolution | | 51 HRUs (R) | 5218 HRUs (M) | 100 × 100 m (A) |
| | | 30 SC (R) | 221 SC (M) | 10 SC (A) |
| | | 29 HRUs (A) | 5270 HRUs (R) | 400 × 400 m (M) |
| | | 10 SC (A) | 85 SC (R) | 11 SC (M) |

each catchment. The projected precipitation change is the most uncertain variable (Fig. 3). Here, the different ensemble members span a wide range. While WRF predicts for all catchments and both half-years an increase of precipitation between 6.3% and 12%, CLM simulates positive and negative trends. This is both due to the different GCMs used and to the different realizations of ECHAM5. Note also that CLM and WRF do not necessarily agree on the sign of projected changes although driven by the same GCM (Wagner et al. 2013). Especially for the summer half-year in the Ammer catchment, all CLM simulations show decreasing rainfall tendencies, but WRF projects increasing precipitation. Considering the ensemble means, for the Ammer catchment increasing precipitation in winter and slightly decreasing rainfall during summer are projected. Also, for Mulde and Ruhr precipitation in winter is projected to increase. During summer precipitation amounts seem fairly stable for the two northern catchments.

For temperature an increase of about 1°C is projected for all catchments, with small variations over the year. While relative humidity values are projected to stay at the current level (range from −1% to 1%), shortwave incoming radiation will be reduced in the scenario period, more pronounced in winter possibly owing to increased cloudiness.

## 4. Hydrological models and their calibration/validation results

The three applied hydrological models are the Precipitation Runoff Modeling System (PRMS; Leavesley et al. 1983) for simulating Ammer and Ruhr, Soil and Water Integrated Model (SWIM; Krysanova et al. 1998) for Mulde and Ruhr, and Water Balance Simulation Model–Eidgenössische Technische Hochschule (WaSiM-ETH; Schulla and Jasper 2007) for Ammer and Mulde. All three are deterministic models, where PRMS and SWIM have a semidistributed approach by dividing the watershed into areas with common hydrological properties [hydrological response units (HRUs)] and WaSiM-ETH is fully distributed with equally sized grid cells, determined by the user. The complexities of the models differ with respect to the required input data, the calculation of terrestrial water balance variables (e.g., evapotranspiration, interception, and infiltration), and the spatial and temporal resolution. Driving meteorological input parameters for each HM and their applied temporal and spatial resolution are shown in Table 4. WaSiM-ETH uses daily and hourly input data; SWIM and PRMS simulate discharge only in daily resolution. For the SWIM model observed precipitation data were corrected for undercatch errors depending on wind speed and the aggregation state of the precipitation (Yang et al. 1999). This procedure is called undercatch correction, resulting in higher precipitation values. PRMS and WaSiM-ETH make use of the observed precipitation data as was applied in its usual way in each model. All three models have a modular structure with components for, for example, evapotranspiration, infiltration, and groundwater modeling. However, they have different calculation schemes. For example, potential evaporation is calculated after Haude (Haude 1952) by PRMS, Priestley–Taylor (Priestley and Taylor 1972) by SWIM, or Penman–Monteith (Monteith 1975) by WaSiM-ETH. For each hydrological model and catchment, an individual setting of parameters, methods, and calculation schemes was developed to assure reasonable and trustable HM calibration results.

TABLE 5. Observational meteorological variables for HM calibration: temperature ($T$), precipitation ($P$), relative humidity (RH), downward shortwave radiation (SW), and wind speed ($W$).

| Catchment | HM | Variables | Source |
|---|---|---|---|
| Ammer | WaSiM | Hourly data of $T$, $P$, SW, RH, $W$ (2002–09) | DWD |
| | PRMS | Daily data of $T$, $P$, RH (1971–2000) | DWD/PIK |
| Mulde | SWIM | Daily data of $T$, $P$, SW, RH (1971–2000) | DWD/PIK |
| | WaSiM | Daily data of $T$, $P$, SW, RH, $W$ (1971–2000) | DWD/PIK |
| Ruhr | PRMS | Daily data of $T$, $P$, RH (1971–2000) | DWD/PIK |
| | | Daily, hourly/8-hourly data of $T$, $P$, RH (1961–96) | DWD/Ruhrverband |
| | SWIM | Daily data of $T$, $P$, SW, RH (1971–2000) | DWD/PIK |

Calibrations of the hydrological models were performed by means of shuffled complex evolution algorithms (Duan et al. 1992; Pakosch 2011) and/or manually. The performances of the models were evaluated visually with respect to daily/hourly flows, mean (MQ) and maximum monthly (MHQ) flow regimes, mean and maximum annual discharges, as well as using efficiency criteria. The applied performance criteria are the Nash–Sutcliffe efficiency (NSE; Nash and Sutcliffe 1970), a modified Nash–Sutcliffe coefficient (modNSE) with a stronger focus on high flows, and the volume bias (VB). The criteria are defined as follows:

$$\mathrm{NSE} = 1 - \frac{\sum_{t=1}^{T} (Q_o^t - Q_s^t)^2}{\sum_{t=1}^{T} (Q_o^t - \overline{Q_o})^2}, \tag{1}$$

$$\mathrm{modNSE} = 1 - \frac{\sum_{t=1}^{T} [(Q_o^t - Q_s^t)Q_o^t]^2}{\sum_{t=1}^{T} [(Q_o^t - \overline{Q_o})Q_o^t]^2}, \tag{2}$$

$$\mathrm{VB} = \frac{\sum_{t=1}^{T} Q_s^t}{\sum_{t=1}^{T} Q_o^t} \tag{3}$$

in which $Q_o$ is observed discharge, $Q_s$ simulated discharge, and $t$ is time. The range of NSE and modNSE is $(-\infty, 1)$, where 1 represents the perfect accordance of the simulated with the observed data, 0 means that the simulations are as accurate as the mean of the observations, and negative values imply that the observed mean is a better predictor than the HM; VB indicates over- and underestimations.

The hydrological models were calibrated to observed discharge data at several gauges in each catchment, driven by observational meteorological data. The principally applied database for calibration is DWD/PIK (see Table 5). This set of data—containing precipitation, temperature, relative humidity, solar radiation, and wind speed—provides the best background for a robust and consistent calibration at all three catchments. A combination of the REGNIE precipitation data—used for the RCM bias correction—and the DWD/PIK data would lead to inconsistent HM calibration results, in particular for the most southern subcatchments of the Ammer catchment owing to overestimations of precipitation by the REGNIE data.

For the calibration and validation process, the split-sample test method was applied for all models. Using different temporal parts of a dataset for calibration and validation allows one to assess the transferability of the calibration results to other time periods. The HMs run, in general, on a daily time step. For the Ammer catchment, WaSiM-ETH simulations performed much better on an hourly simulation time step compared to a daily time step because of the small catchment size and the alpine character. Meteorological data on an hourly time step were only available for the years 2002–09, which restricted the calibration and validation to this time period. The following RCM simulations were then also made in the hourly resolution.

Figure 4 displays the mean monthly discharge (MQ) and mean maximum monthly discharge (MHQ) flow characteristics for measured runoff data and simulations based on observed meteorological data (SimObs), used for calibration and validation. Figures 4a and 4e show the results of the hourly Ammer simulation from 2002 to 2009, as Figs. 4b and 4f show the simulations with daily Ammer data simulated by PRMS for the control period from 1971 to 2000. Both HMs simulate the annual cycle of MQ well with a slight overestimation in April, more pronounced by the daily PRMS simulation in Fig. 4b. The MHQ is also well simulated by both models: the high flood peak in August of the measured data in Fig. 4e is the result of a severe flood event in 2005. Figures 4c and 4g illustrate the results of the Mulde calibration by SWIM and WaSiM-ETH. While SWIM overestimates

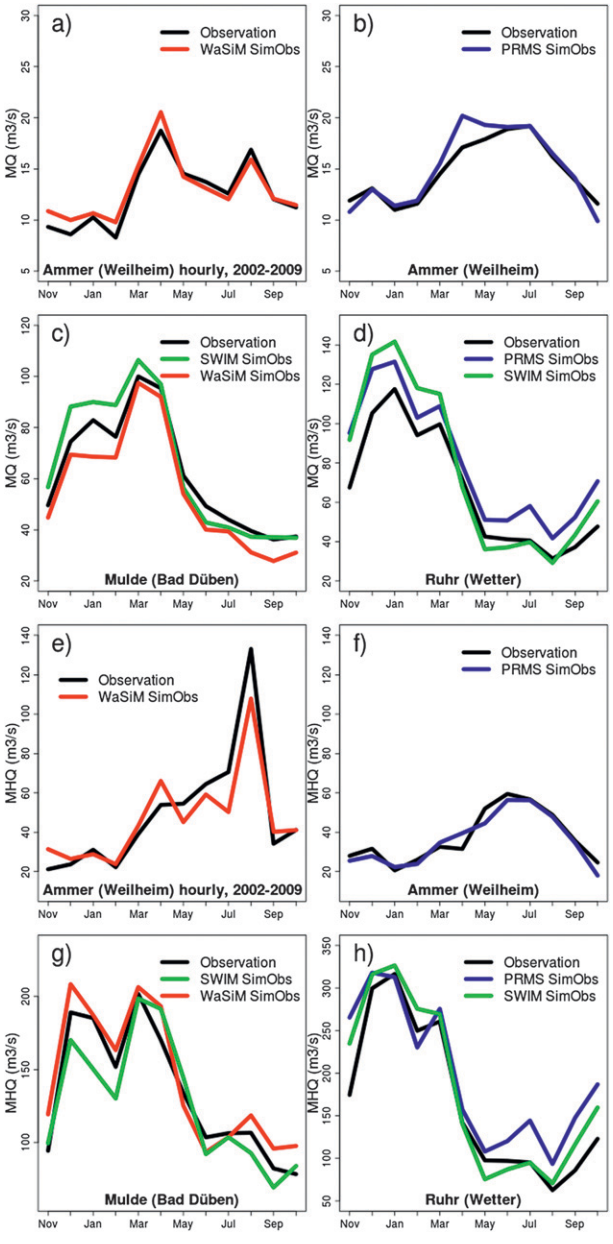


FIG. 4. Mean (MQ) and mean maximum monthly (MHQ) flows of observed runoff and HM simulations based on meteorological station data (SimObs).

MQ during winter and underestimates it in summer, WaSiM-ETH underestimates the runoff over the entire year. The MHQ discharge, however, is overestimated by WaSiM-ETH and underestimated by SWIM. The hydrological cycle for the Ruhr is shown in Figs. 4d and 4h. Both PRMS and SWIM overestimate MQ during winter, and PRMS also for summer. The MHQs are well simulated with a slight overestimation during summer by PRMS.

TABLE 6. Calibration performance of the HMs for the Ammer, Mulde, and Ruhr catchments. The Nash–Sutcliffe efficiency (NSE), modified Nash–Sutcliffe coefficient (MmodNSE), and volume bias (VB) are shown for the calibration (Cal) and validation (Val) periods.

| | | NSE | | ModNSE | | VB | |
|---|---|---|---|---|---|---|---|
| Gauge | Model | Cal | Val | Cal | Val | Cal | Val |
| | | | | Ammer | | | |
| Weilheim | WaSiM | 0.87 | 0.72 | 0.95 | 0.90 | −2% | 11% |
| | PRMS | 0.78 | 0.68 | 0.90 | 0.71 | −1% | 3% |
| | | | | Mulde | | | |
| Bad Düben | SWIM | 0.77 | 0.79 | 0.90 | 0.85 | 7% | 4% |
| | WaSiM | 0.79 | 0.82 | 0.86 | 0.94 | −12% | −10% |
| | | | | Ruhr | | | |
| Wetter | PRMS | 0.82 | 0.71 | 0.91 | 0.91 | 15% | 24% |
| | SWIM | 0.88 | 0.80 | 0.96 | 0.94 | 16% | 15% |

Table 6 gives an overview of the performance criteria within the calibration and validation periods for the downstream gauges Weilheim, Bad Düben, and Wetter of the three catchments investigated. The HMs attain for the calibration periods (cal) NSE values between 0.77 and 0.88, and modNSE reaches high values from 0.86 to 0.96. The volume bias indicates general over- and underestimations. In the case of gauge Weilheim in the Ammer catchment, there are nearly no volume differences between observations and simulations for the calibration periods. SWIM simulates the runoff volume of the Mulde better than WaSiM-ETH, and the volume for gauge Wetter of the Ruhr is overestimated by both HMs. The stronger overestimations in the Ruhr catchment are at least partly due to water abstractions that were not considered in the simulations. The comparison of the calibration with the validation periods shows that for most cases no large impairments occur for the Mulde and Ruhr catchments, but the small alpine Ammer catchment shows less transferability of the calibrated parameters to other time periods.

## 5. Climate change impact on hydrology

This section discusses the impact of climate change on the hydrology of the three catchments. First, the hydrological simulations driven by observed meteorological data are compared to the simulations driven by the bias-corrected RCM input with 7-km spatial resolution for the 30-yr control period from 1971 to 2000. This allows evaluation of the RCM data as input for the HMs. Second, the resulting discharges of the high-resolution RCM input for the control period 1971–2000 and the

scenario period 2021–50 are compared to assess the impact of climate change on hydrology.

### *a. Control period*

Figure 5 shows the MQ (left) and MHQ (right) results of the simulations driven by observed meteorological data and the RCM simulation results for the control period 1971–2000.

#### 1) AMMER

Precipitation is overestimated by the RCMs at the Ammer catchment throughout the year. In winter the discharge is not directly affected by these precipitation overestimations, as precipitation contributes mainly to snow storage. Thus, the simulated runoff at gauge Weilheim based on RCM input from November until March is close to the simulations with observed meteorological data (SimObs) (see Fig. 5, top). However, the RCM precipitation causes an overestimation of the snow storage which is 2–3 times larger than the simulated one for SimObs (not shown). For the rest of the year, discharge in the Ammer is overestimated by the CLM-driven simulations owing to higher precipitation amounts and the additional snowmelt in spring and early summer. For example in May, around 20% of total runoff of the SimObs simulations originates from snowmelt, whereas for the RCM-driven simulations the portion of the snow storage on total runoff is still 45%–60%. The WRF-driven simulation generates considerably lower discharges than the CLM ones. This is because, first, a minor overestimation of precipitation and, thus, less overestimation of snow storage in winter and, second, the underestimated relative humidity causes high evaporation rates leading to a markedly reduced runoff during summer.

A sensitivity test of relative humidity (RH) with CLM and WRF-RH input data is presented in Fig. 6. When the original WRF-RH data is replaced by the CLM-RH and all other input variables like precipitation and temperature are unchanged (red), MQ draws near to the original CLM simulation (green), but keeps its characteristic peak flow in May from the WRF simulation. The contrary behavior occurs when the relative humidity of WRF replaces the CLM-RH (blue). This indicates the large influence of RH and partly explains the differences of up to $15\,m^3\,s^{-1}$ during summer and autumn in the simulations of the Ammer catchment with WaSiM-ETH. PRMS does not react as strongly to the input parameter of humidity at gauge Weilheim. While the overestimation of the CLM-driven simulations for both HMs, WaSiM-ETH, and PRMS are similar for mean monthly discharges, maximum monthly discharges shown in Fig. 5 (top right) are, in particular, overestimated more in summer by WaSiM-ETH than by PRMS.

#### 2) MULDE

At the downstream gauge Bad Düben in the Mulde catchment (Fig. 5, middle), the individual RCM simulations for the control period also differ. The simulations driven by WRF induce the lowest mean monthly discharges. The climate input from CLM mostly results in an overestimation. This overestimation is more pronounced in summer and stronger for the WaSiM-ETH simulations. That also applies to the mean maximum monthly discharge. There are several reasons for the deviations between the simulations with observations and climate input from the RCMs: The undercatch-corrected precipitation data used during calibration of the SWIM model are higher than for the REGNIE data, which were applied for bias correction of the RCM precipitation. This is more pronounced during winter when the measurement errors of snow are adjusted. The underestimation of discharge by WaSiM-ETH with WRF climate input in summer is comparable with the situation in the Ammer catchment, likely owing to the underestimation of humidity by WRF in summer. The overestimation of discharge in the simulations with CLM climate input can be attributed to the overestimation of humidity and underestimation of radiation by CLM. The overestimation is stronger in the simulations with WaSiM-ETH. In the simulations with SWIM, the factors resulting in a lower discharge (lower precipitation input than for calibration) and higher discharge (higher humidity and lower radiation) partly compensate and, thus, lead to more moderate discharge overestimations. The overestimation of discharge driven by CLM climate input is larger during the summer than the winter months. This is probably due to the effect of evapotranspiration (which is reduced by the lower radiation and higher humidity) that is stronger during the summer months. The CLM-driven runs show a noticeable peak in August, which cannot be explained by the mean monthly precipitation sums, an extreme precipitation event, or the calculated evaporation rates. A further analysis of mean 3-day maximum precipitation sums showed that the peak most likely results from higher precipitation intensities than in the observed data (analysis not shown here).

#### 3) RUHR

Figure 5 (bottom) shows the MQ and MHQ results for the gauge Wetter. While the single SWIM simulations are comparable and fit the seasonal cycle, given by the SimObs curve well, the single RCM results of PRMS vary widely. The PRMS-WRF–driven simulation conforms

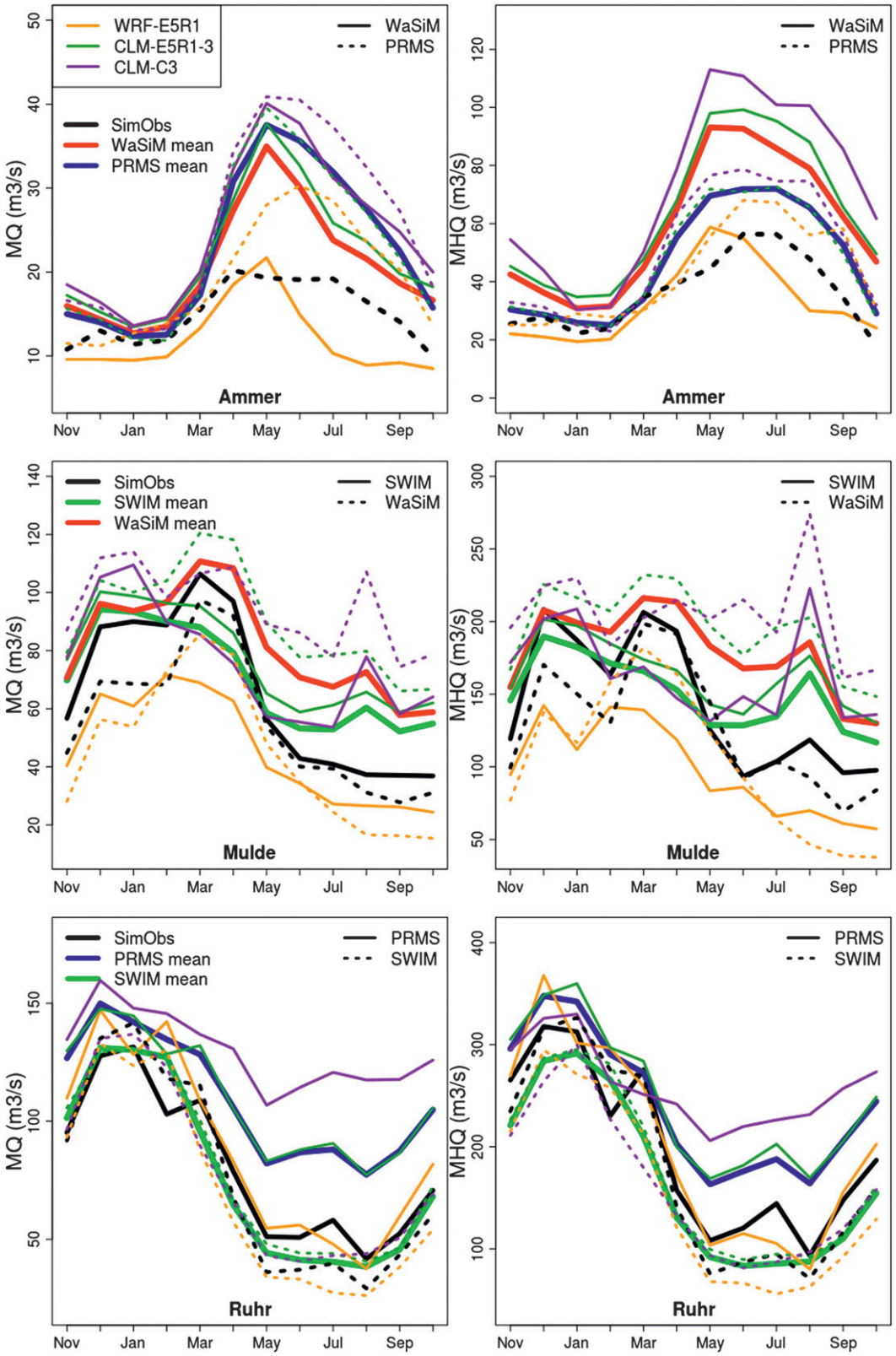


FIG. 5. (left) MQ and (right) MHQ flows for the control period 1971–2000. Simulations are based on measured meteorological data (SimObs) and RCM results for both HMs at the three investigated catchments.

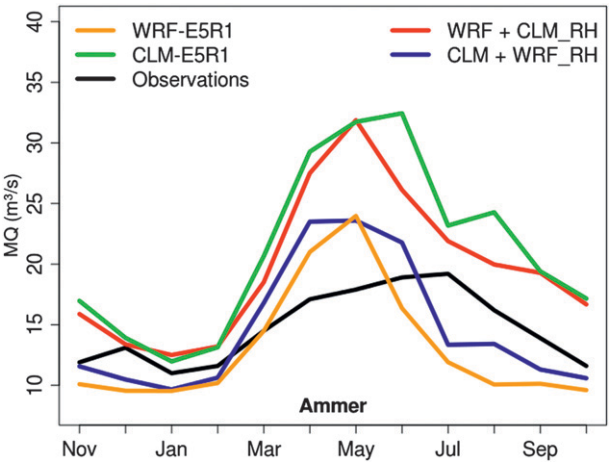


FIG. 6. Sensitivity test of the influence of RH to the discharge simulations with WaSiM-ETH in the Ammer catchment using CLM and WRF input for the control period 1971–2000.

to the simulation driven by observed meteorological data. In contrast, the CLM simulations and, in particular, the discharge resulting from the CLM-C3 combination (purple) have a too small seasonal cycle, inducing overestimation of low flow conditions during summer, more pronounced for MQ. The overestimation of discharge in summer by PRMS is, comparable to the Ammer simulations, induced by the overestimation of RH. SWIM does not react as strongly to RH in summer at gauge Wetter.

### *b. Scenario period*

To investigate possible future changes in discharge and flood hazard, the percentage changes in MQ and MHQ between the scenario (2021–50) and control period (1971–2000) are shown in Fig. 7 for all three catchments.

#### 1) AMMER

The Ammer catchment shows tendencies of increasing mean monthly discharge in winter and decreasing discharge during summer for the scenario period (see Fig. 7, top left). WaSiM-ETH predicts a more pronounced trend in winter than PRMS. The spread of the single ensemble members is large for both hydrological models, so a reliable statement about a future change in discharge is not possible. The WRF-PRMS simulation is the only one that reacts in the opposite way to the other RCMs in winter. The reason for this exceptional reaction in PRMS could not be fully explained. At this point the WaSiM-ETH results are more plausible, reflecting the change in WRF-precipitation input with increasing values over the entire year except for December, January, and June. To detect a trend for MHQ is even more difficult (see Fig. 7, top right), as the differences of the ensemble members are larger than for MQ. The single ensemble members show, in most cases, the same discharge tendencies as for the mean monthly discharge. For the ensemble mean, increasing tendencies of peak flows are projected in winter, while decreasing trends can be found in August and September. The projected mean changes would induce a flattening of the annual discharge cycle at the alpine Ammer catchment. The combination of higher temperatures and, thus, more precipitation falling as rain in winter will increase discharge and also induce an earlier beginning of the snowmelt season. In summer, reduced projected rainfall (except WRF) and higher temperatures, hence higher evaporation, leads to lower runoffs.

#### 2) MULDE

The projected slight future increase of precipitation in the Mulde catchment almost throughout the whole year is reflected by changes in simulated discharge between the scenario and control period for the different ensemble members (Fig. 7, middle). The simulation with the WRF-E5 climate input shows an increase in discharge in nearly all months, consistent with the change in precipitation for this ensemble member. The CLM simulation results cause heterogeneous future change signals. In August, the CLM results show the most notable decline of runoff, most likely owing to lower precipitation intensities than in the control period. For example, for CLM-C3, the intensities in August are higher than in July for the control run, despite comparable mean precipitation sums. In the scenario period, the difference between July and August precipitation intensities are smaller than for the control period (control: 15%, scenario: 9%), and the total intensities are also lower (decrease of 6% in July and 12% in August); thus, the discharge peak in August is absent in the future period (analysis not shown here).

#### 3) RUHR

For the Ruhr catchment, the ensemble spread of MQ and MHQ is large at gauge Wetter (Fig. 7, bottom). The ensemble mean projects an increase of runoff for most of the year except for August, October (MQ and MHQ), and January (MQ). In contrast to the Ammer catchment, the annual cycle of the Ruhr will be intensified. PRMS and SWIM show a comparable and consistent picture for the single RCM results. Similar to the Ammer and Mulde catchments, WRF results in increasing discharges and flood tendencies in summer for the scenario period. The simulations based on the Community Land Model show signals of increasing and decreasing mean and maximum monthly discharge values.

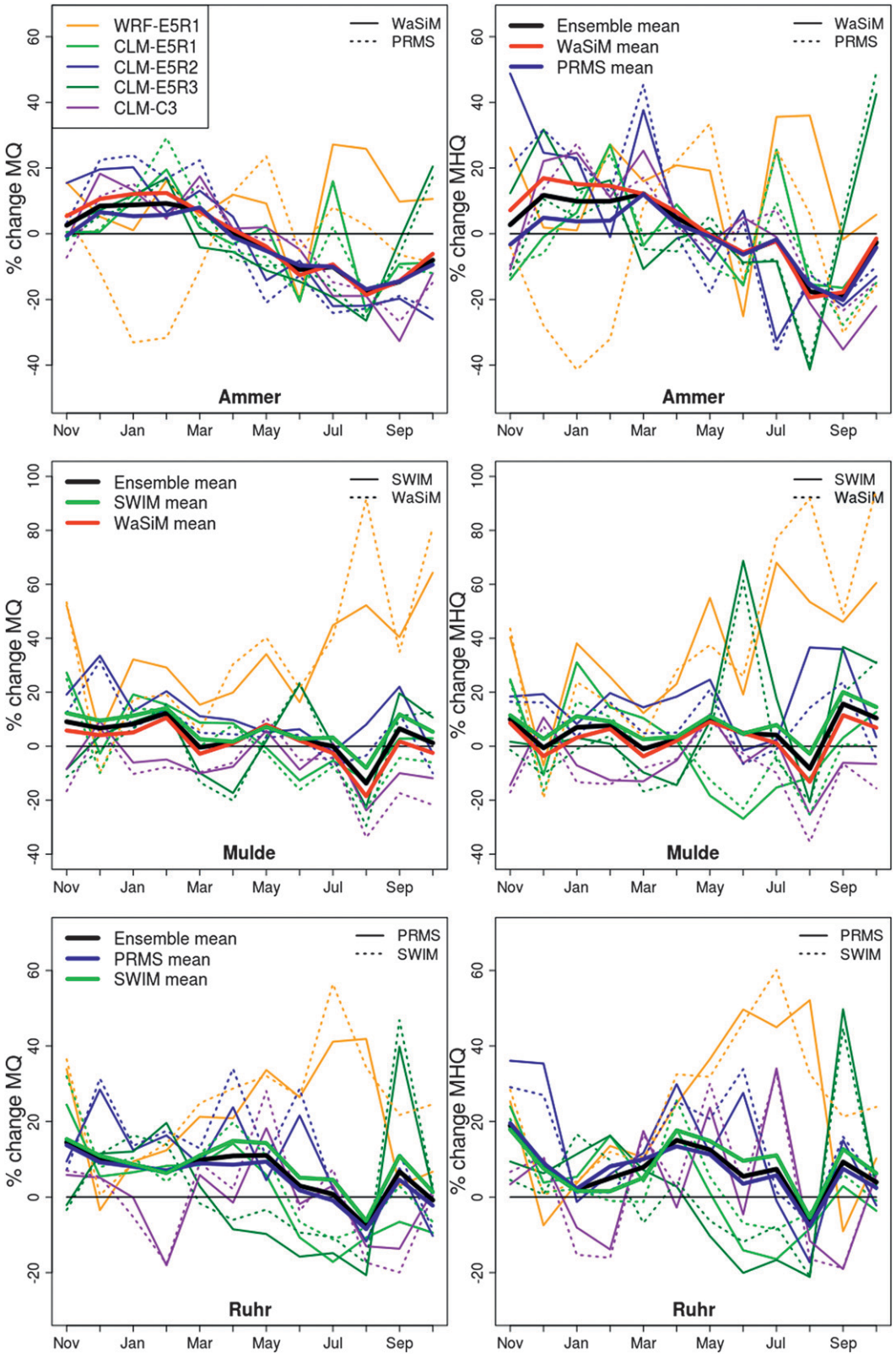


FIG. 7. Percentage difference of (left) MQ and (right) MHQ flows between the scenario (2021–50) and control (1971–2000) period.

The resulting impacts of climate change on regional hydrology, and particularly with regard to flood probability, are subject to intensive research. For the twenty-first century, studies have shown heterogeneous results for discharge changes and extreme flood events in Germany, for example, for our three catchments of investigation (Menzel and Burger 2002; Kunstmann et al. 2004; Morgenschweis et al. 2007). Menzel and Burger (2002) investigated the runoff changes of the Mulde river in eastern Germany for the next hundred years and ascertained a clear tendency of decreasing precipitation and thus reduced discharges for this catchment. These results are based on a single-model chain with one downscaled GCM driving a single HM. Our multimodel study gives contrary conclusions, beginning with precipitation signals that are highly different depending on the chosen climate model in this catchment. Both increasing and decreasing precipitation projections cause slightly higher mean runoffs at the Mulde. Kunstmann et al. (2004) made a single-model study for the alpine Ammer catchment in the south of Germany. Increased simulated evaporation rates in summer thereby induce a reduction of summer runoff, and warmer winter temperatures yield to higher discharge owing to a reduced snow–rain ratio. Unlike the preceding climate change study, the general trends found by Kunstmann et al. can be confirmed by our modeling results. Morgenschweis et al. (2007) studied the impact of climate change on the management of the reservoirs in the Ruhr catchment. The impact study is based on an ensemble strategy with one RCM, one river basin model, and three common SRES scenarios. They found that runoff remains at roughly the same level for the A1B scenario during the period 2011–70 compared to their reference period 1961–95. Only for the last investigated time period (2071–2100) did they detect decreasing runoff tendencies in autumn and increased runoff during the winter months owing to intensified rainfall. In our multimodel study, considerably rising discharges in winter are, however, already projected until the year 2050. Also, the autumnal decrease of discharge with up to 40% can not be confirmed by our results. However, our modeling results are affected by uncertainties arising from the use of various datasets for the HM calibration and the RCM bias correction, individual configurations of model calibration, and the model chain by itself.

### c. *Uncertainties within the model chain*

The large differences within the projected change signals for all three catchments raise the question about the sources of uncertainties within the model chain. For this purpose, the influence of the four model chain members (GCMs, different realizations, RCMs, and HMs) are analyzed and compared. Our ensemble consists of five RCM simulations and 10 hydrological simulations for each catchment and is therefore too small for an extensive quantitative statistical analysis. However, it permits a qualitative estimation of the ensemble spread and the contribution of GCMs, RCMs, and HMs to this spread.

The relative changes in discharge for given return periods are shown in Fig. 8. This is performed with the plotting position method, showing the future relation between return periods and the relative change of return values, determined by the annual, winter, and summer maximum discharge values. The return value changes are divided into the single RCM results and one color represents both HMs. The wide spread of the single simulation results, already ascertained by the MQ and MHQ changes, is reconfirmed by the return value changes. The variability of the change signals is most pronounced in the Mulde catchment, with a wide spread of positive and negative signals. It is striking that the results of one RCM are mostly close together; however, the RCMs among each other differ considerably. This is not only valid for different RCMs, for example, at the Mulde catchment in the summer half-year, when WRF (orange) and CLM (dark green) project opposite change signals, but also for different realizations of one RCM (e.g., first and second realizations of CLM in winter at the Mulde and Ammer). The differences between the three realizations of the CLM RCM also entail discrepancies among the simulations driven by different GCMs. Figure 9 shows the same method and results as Fig. 8, but grouped according to the single hydrological model results. The mean change signals of the HMs are close together, and the single HMs do not show divergent change signals in contrast to the climate model results. The only exception is the winter half-year at the Ammer, when WaSiM-ETH and PRMS do not agree for return periods shorter than 5 yr. Analysis of Figs. 8 and 9 indicates a minor impact of the HMs on the overall uncertainty within the applied model chain, in contrast to the climate models.

To further estimate which model chain member causes the largest contribution to the overall variability, the particular variabilities of the projections for the future changes are compared. Here, the projected climate change signals of MHQ are analyzed. The results based on MQ (not mentioned here) show comparable results. For the analysis, the ensemble is divided into four groups. The first group represents the uncertainties produced by the GCMs. The changes in MHQ between the scenario and control period of the CLM simulations driven by the GCMs ECHAM5 and CCCma3 are examined. If the two different GCMs yield similar

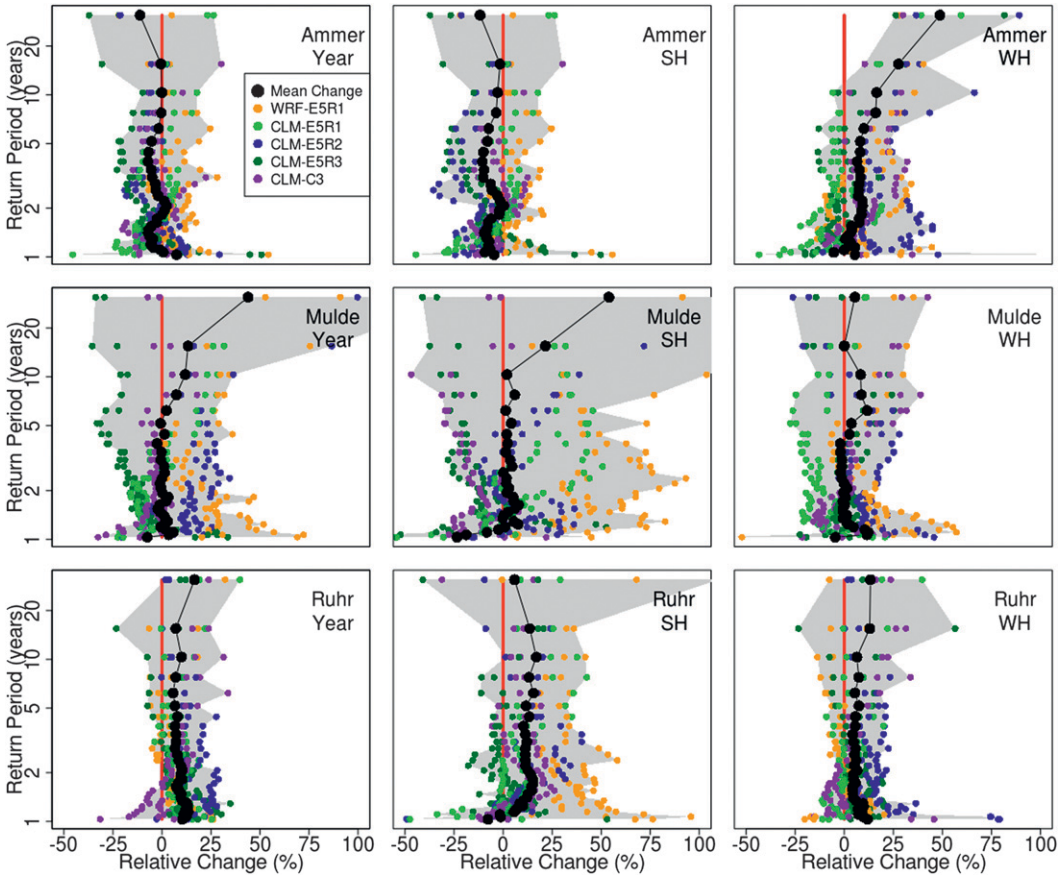


FIG. 8. Changes in discharge for given return periods based on change of the maximum annual, summer half-year (SH) or winter half-year (WH) values (2021–50 and 1971–2000). The gray shaded areas mark the maximum range of the single ensemble members (maximum of shaded area for Mulde/year, 153%; Mulde/SH, 286%; and Ruhr/SH, 108%). One color implies both HMs.

(different) change signals under the same conditions (same gauge, realization, and HM), the range of variability and therefore the resulting uncertainty is small (large). The second group represents the natural variability of the projections and consists of the three different realizations of ECHAM5, downscaled by CLM. The uncertainties produced by the RCMs is represented by the WRF and CLM simulations driven by the first realization of ECHAM5, in group three. The fourth group consists of the differences of the projected future changes in MHQ, caused by the different HMs. To test whether the groups differ from each other, two common methods were applied: analysis of variance (ANOVA) (Morrison 1967) as a parametric and Kruskal–Wallis (K-W) (Kruskal and Wallis 1952) as a nonparametric statistical test. The applicability of both test schemes was assured by testing the distributions of the formed groups (not shown). Table 7 shows the resulting $p$ values of the two tests. Low values indicate more significant differences between the tested groups and, thus, a high proportion to the uncertainty within the model chain.

The largest contribution to the overall uncertainty in summer results from the two different RCMs, followed by the GCMs and their realizations together with the three HMs. The large influence of the RCMs on the future runoff in summer is not unexpected, as WRF and CLM show almost always divergent future changes of precipitation, which is the most important factor for discharge. As seen in Wagner et al. (2013), the climate change signals of the CLM-E5R1 and WRF-E5R1 differ substantially over the whole region of Germany; thus, small shifts in the patterns over the catchments is not enough to explain this. However, there are important differences between the two models that can have an impact, for example, the convection parameterization, as different parameterizations can have different soil-moisture feedback sensitivities.

In winter, the main uncertainties result from natural variability, depending on the statistical test, followed by

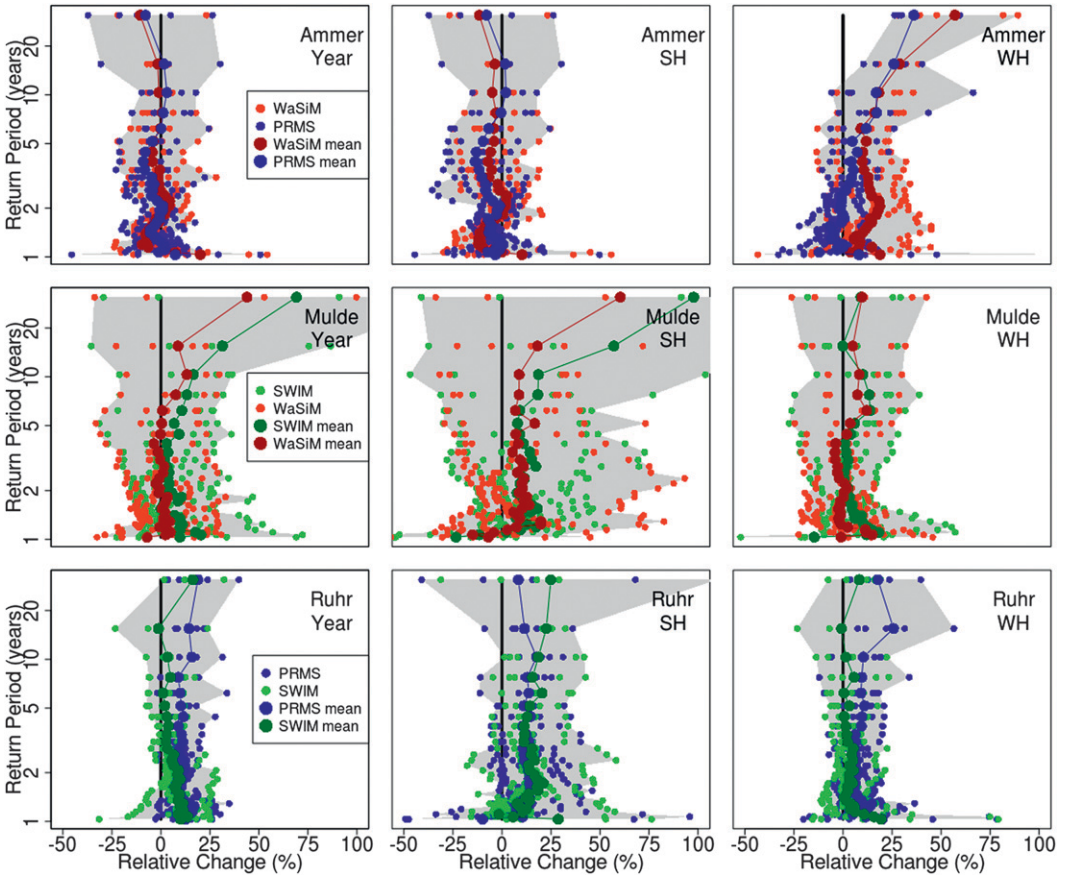


FIG. 9. As in Fig. 8 but one color implies one HM and all RCMs.

the RCMs (K-W) or the GCMs (ANOVA). The uncertainty in winter is not much affected by the HMs. As the RCM and GCM groups are especially underrepresented in our study, the results of the applied statistical tests should not be overrated. They confirm the already detected arrangement of uncertainty sources by means of visual analysis of Figs. 7, 8, and 9.

However, the majority of previous studies about uncertainties in multimodel impact studies confirm the small contribution of the HMs to the overall variability of results (Andréasson et al. 2004; Wilby and Harris 2006). The latter investigated the impact of climate change on low flows at the Thames using four GCMs, two emission scenarios, two different statistical downscaling methods, and two HM structures with two different parameter sets. They found that the GCMs cause the largest uncertainty, followed by the downscaling method and emission scenarios and, finally, the HMs. Kay et al. (2008) confirm the important role of the global models within a multimodel impact study, investigating changing flood frequencies in England with five GCMs, four emission scenarios, statistically and dynamically downscaled data, and two HMs with different calibration sets. But they also point out that natural variability plays an important role for the uncertainty and that the global models are as important as they are in this study because one of the five models predicts, in contrast to the other applied models, large increases in winter rainfall. That natural variability can cause more uncertainty than different climate models within a model chain is also tested by Booij (2005), who explored changes in flood frequency at the Meuse in western Europe. A study by Huang et al. (2013) confirms the

TABLE 7. The *p* values of the statistical tests ANOVA and K-W for the winter (WH) and summer (SH) half-year. Low values indicate a high proportion to the overall uncertainty.

| | WH | | SH | |
|---|---|---|---|---|
| | ANOVA | K-W | ANOVA | K-W |
| GCM | 0.11 | 0.11 | 0.08 | 0.09 |
| Realizations | 0.00 | 0.00 | 0.19 | 0.22 |
| RCM | 0.37 | 0.08 | 0.00 | 0.00 |
| HM | 0.99 | 0.98 | 0.26 | 0.21 |

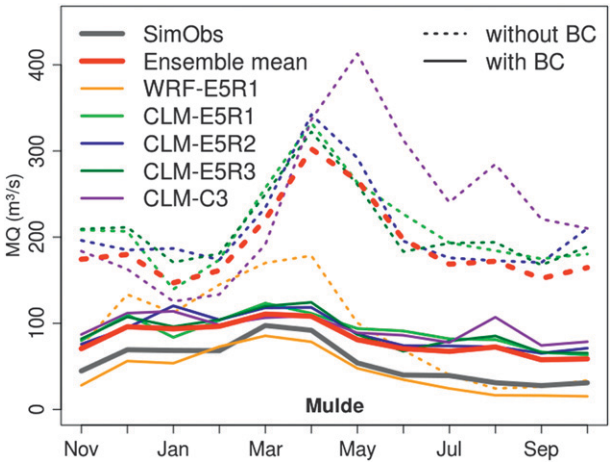


FIG. 10. Effect of the bias-corrected (BC) precipitation and temperature data on the mean monthly discharge (1971–2000) at gauge Bad Düben, Mulde: simulations based on WaSiM-ETH.

high influence of the use of different RCMs on the overall uncertainty. With two dynamically and one statistically downscaled RCMs and three emission scenarios driving the SWIM model, they investigated climate change impacts on river flood conditions for the five largest river basins in Germany. They were faced with highly divergent hydrological simulation projections and assigned the major uncertainty in this study to the use of different kinds of RCMs.

## 6. Discussion and conclusions

This study investigated the projected changes of discharge together with the associated uncertainty of three small- to medium-sized catchments in Germany for the near future. The future period 2021–50 was chosen for its planning relevance and its relative independence from uncertain scenario assumptions about future greenhouse gas emissions. However, the choice of the near-future scenario implies a weaker climate change signal and the 30-yr time period impedes statistical analyses of extreme values.

The single hydrological model simulations in our study produce varying change signals, and the range of the different RCM-based simulations is very large and prohibits a clear estimation about future changes of flood discharge in Germany. The large spread of the climate models transfers to the hydrological simulation results. The necessity of a bias correction of the meteorological model input for the hydrological impact analysis is shown in Fig. 10 for the mean monthly discharge at gauge Bad Düben (Mulde). The simulations without bias-corrected input exceed the observed discharge up to 4 times and also overestimate the seasonal cycle. An additional possibility to counter the meteorological biases could be to correct the biases of the GCMs. Xu and Yang (2012) successfully developed an improved dynamical downscaling method (IDD) that corrects, after downscaling by a RCM, the climatological means, extreme events, and probability distributions for various variables like temperature, precipitation, wind vectors, and moisture. Such a method could prevent the introduction of additional biases within the model chain and, for example, circumvent the over- and underestimations of runoff in the hydrological modeling resulting from biased humidity values. This method, however, does not guarantee bias-free data (RCM bias is still there), and it is unclear how climate change signals are affected. The biases, and bias correction, can have large impacts on the results, and it is important to work with decreasing biases in simulations and simultaneously with conservative bias correction as an intermediary step (e.g., Xu and Yang 2012; Berg et al. 2012; Piani and Haerter 2012).

Despite the relatively small size of the ensemble, our study permits an estimation of the range of results—especially in comparison to single-model studies—and also an attribution of the different sources of uncertainty in a qualitative way. Within our project, the restricted number of suitable GCMs and the computational demands of the simulations inhibited a larger ensemble. Nevertheless, this is one of the largest currently available concerted RCM-based ensembles at such a high resolution. The analysis of our ensemble showed that for the climate change signal, the main uncertainties within the model chain result from the RCMs, especially in summer. In winter, the natural variability, represented by the three realizations of ECHAM5, cause the highest contribution to the uncertainty. The impact of the HMs mostly plays a minor role. Furthermore, our study confirms the necessity of a multimodel approach throughout the modeling chain. The results demonstrate that single simulations can be quite misleading and that small ensembles can give qualitative and limited quantitative indications of the existence and uncertainty range of the change signal.

*Acknowledgments.* This work was funded and performed within the CEDIM project "Flood Hazards in a Changing Climate." The support is gratefully acknowledged. We also thank the modeling groups of the global climate models ECHAM5 and CCCma3 and the regional climate models CLM and WRF, as well as the developers of the hydrological models SWIM, PRMS, and WaSiM-ETH. We also appreciate the work of the R Development Core Team. Also gratefully acknowledged are the Deutscher Wetterdienst

(DWD), the Wasserwirtschaftsamt (WWA) Weilheim, the Hochwassernachrichtendienst (HND) Bayern, the Landestalsperrenverwaltung Sachsen (LTV), and the Ruhrverband for providing meteorological and hydrological data. We also want to thank the Sächsisches Landesamt für Umwelt, Landwirtschaft und Geologie (LfULG), the Bundesamt für Kartographie und Geodäsie (BKG), the Bundesamt für Geowissenschaften und Rohstoffe (BGR), the Landesamt für Natur, Umwelt und Verbraucherschutz (LANUV) NRW, the Geologischer Dienst NRW, and the RAPHAEL project. We also acknowledge the suggestions from two anonymous reviewers that helped us greatly in improving the manuscript.

## REFERENCES

Andréasson, J., S. Bergstroem, B. Carlsson, L. P. Graham, and G. Lindstroem, 2004: Hydrological change-climate change impact simulations for Sweden. *Ambio,* **33,** 228–234.

Berg, P., H. Feldmann, and H.-J. Panitz, 2012: Bias correction of high resolution regional climate model data. *J. Hydrol.,* **448–449,** 80–92.

——, S. Wagner, H. Kunstmann, and G. Schädler, 2013: High resolution regional climate model simulations for Germany: Part I—Validation. *Climate Dyn.,* **40,** 401–414, doi:10.1007/s00382-012-1508-8.

Beurton, S., and A. H. Thieken, 2009: Seasonality of floods in Germany. *Hydrol. Sci. J.,* **54,** 62–76.

Booij, M. J., 2005: Impact of climate change on river flooding assessed with different spatial model resolutions. *J. Hydrol.,* **303,** 176–198.

Christensen, J. H., and Coauthors, 2007: Regional climate projections. *Climate Change 2007: The Physical Science Basis,* S. Solomon et al., Eds., Cambridge University Press, 847–940.

Dankers, R., and L. Feyen, 2008: Climate change impact on flood hazard in Europe: An assessment based on high-resolution climate simulations. *J. Geophys. Res.,* **113,** D19105, doi:10.1029/2007JD009719.

Deser, C., A. Phillips, V. Bourdette, and H. Teng, 2012: Uncertainty in climate change projections: The role of the internal variability. *Climate Dyn.,* **38,** 527–546.

Doms, G., and U. Schättler, 2002: A description of the nonhydrostatic regional model LM. Part I: Dynamics and numerics. COSMO Rep., Deutscher Wetterdienst, Offenbach, Germany, 140 pp. [Available online at http://www.dwd.de/bvbw/generator/DWDWWW/Content/Forschung/FE1/Veroeffentlichungen/Download/LMdocu__I__dynamics__0211,templateId=raw,property=publicationFile.pdf/LMdocu_I_dynamics_0211.pdf.]

Duan, Q. Y., S. Sorooshian, and V. K. Gupta, 1992: Effective and efficient global optimization for conceptual rainfall-runoff models. *Water Resour. Res.,* **28,** 1015–1031.

Feldmann, H., G. Schädler, H.-J. Panitz, and C. Kottmeier, 2013: Near future changes of extreme precipitation over complex terrain in Central Europe derived from high resolution RCM ensemble simulations. *Int. J. Climatol.,* doi:10.1002/joc.3564, in press.

Graham, L. P., J. Andréasson, and B. Carlsson, 2007: Assessing climate change impacts on hydrology from an ensemble of regional climate models, model scales and linking methods—A case study on the Lule River basin. *Climatic Change,* **81,** 293–307.

Haude, W., 1952: Zur Möglichkeit nachträglicher Bestimmung der Wasserbeanspruchung durch die Luft und ihrer Nachprüfung an Hand von Tropfversuchen und Abflussmessungen. *Ber. Dtsch. Wetterdienstes,* **32,** 27–34.

Haylock, M., N. Hofstra, A. M. G. K. Tank, E. J. Klok, P. D. Jones, and M. New, 2008: A European daily highresolution gridded data set of surface temperature and precipitation for 1950–2006. *J. Geophys. Res.,* **113,** D20119, doi:10.1029/2008JD010201.

Hewitt, C. D., and D. J. Griggs, 2004: Ensembles-based predictions of climate changes and their impacts (ENSEMBLES). ENSEMBLES Tech. Rep. 1, Met Office, United Kingdom, 5 pp. [Available online at http://ensembles-eu.metoffice.com/tech_reports/ETR_1_vn2.pdf.]

Huang, S., F. F. Hattermann, V. Krysanova, and A. Bronstert, 2013: Projections of climate change impacts on river flood conditions in Germany by combining three different RCMs with a regional eco-hydrological model. *Climatic Change,* **116,** 631–663, doi:10.1007/s10584-012-0586-2.

Hurkmans, R., W. Terink, R. Uijlenhoet, P. Torfs, D. Jacob, and P. Troch, 2010: Changes in streamflow dynamics in the Rhine basin under three high-resolution regional climate scenarios. *J. Climate,* **23,** 679–699.

Kay, A. L., H. N. Davies, V. A. Bell, and R. G. Jones, 2008: Comparison of uncertainty sources for climate change impacts: flood frequency in England. *Climatic Change,* **92,** 41–63.

Kleinn, J., C. Frei, J. Gurtz, D. Lüthi, P. L. Vidale, and C. Schär, 2005: Hydrologic simulations in the Rhine basin driven by a regional climate model. *J. Geophys. Res.,* **110,** D04102, doi:10.1029/2004JD005143.

Kruskal, W. H., and W. A. Wallis, 1952: Use of ranks in one-criterion variance analysis. *J. Amer. Stat. Assoc.,* **47,** 583–621.

Krysanova, V., D. Muller-Wohlfeil, and A. Becker, 1998: Development and test of a spatially distributed hydrological/water quality model for mesoscale watersheds. *Ecol. Modell.,* **106,** 261–289.

Kunstmann, H., K. Schneider, R. Forkel, and R. Knoche, 2004: Impact analysis of climate change for an Alpine catchment using high resolution dynamic downscaling of ECHAM4 time slices. *Hydrol. Earth Syst. Sci.,* **8,** 1031–1045.

——, J. Krause, and S. Mayr, 2005: Inverse distributed hydrological modelling of Alpine catchments. *Hydrol. Earth Syst. Sci.,* **2,** 2581–2623.

Leavesley, G. H., R. W. Lichty, B. M. Troutman, and L. G. Saindon, 1983: Precipitation-runoff modeling system: User's manual. USGS Water-Resources Investigations Rep. 83-4238, 206 pp. [Available online at http://pubs.usgs.gov/wri/1983/4238/report.pdf.]

Lorenz, C., and H. Kunstmann, 2012: The hydrological cycle in three state-of-the-art reanalyses: Intercomparison and performance analysis. *J. Hydrometeor.,* **13,** 1397–1420.

Marx, A., H. Kunstmann, A. Bárdossy, and J. Seltmann, 2006: Radar rainfall estimates in an alpine environment using inverse hydrological modelling. *Adv. Geosci.,* **9,** 25–29.

Meehl, G. A., G. J. Boer, C. Covey, M. Latif, and R. J. Stouffer, 2000: The Coupled Model Intercomparison Project (CMIP). *Bull. Amer. Meteor. Soc.,* **81,** 313–318.

Menzel, L., and G. Burger, 2002: Climate change scenarios and runoff response in the Mulde catchment (Southern Elbe, Germany). *J. Hydrol.,* **267,** 53–64.

Monteith, J. L., 1975: *Vegetation and the Atmosphere: Principles.* Academic Press, 278 pp.

Morgenschweis, G., G. zur Strassen, S. Patzke, and D. Schwanenberg, 2007: Estimation of the Impact of Possible Climate Change on the Management of the Reservoirs in the Ruhr Catchment Basin. Annual Rep. Ruhrwassermenge, Ruhrverband, Essen, Germany, 32–50. [Available online at http://www.talsperrenleitzentrale-ruhr.de/daten/internet/veroeffentlichungen/climate_change.pdf.]

Morrison, D., 1967: *Multivariate Statistical Methods.* McGraw-Hill, 338 pp.

Nash, J., and J. Sutcliffe, 1970: River flow forecasting through conceptual models part I—A discussion of principles. *J. Hydrol.,* **10,** 282–290.

Österle, H., F. W. Gerstengarbe, and P. C. Werner, 2006: Ein neuer meteorologischer Datensatz für Deutschland, 1951–2003. Tech. Rep., Potsdam Institut für Klimafolgenforschung, Potsdam, Germany, 3 pp.

Pakosch, S., 2011: Development of a fuzzy rule based expert system for flood forecasts within the meso-scale upper main basin. Ph.D. thesis, University of the Federal Armed Forces, 204 pp.

Piani, C., and J. O. Haerter, 2012: Two dimensional bias correction of temperature and precipitation copulas in climate models. *Geophys. Res. Lett.,* **39,** L20401, doi:10.1029/2012GL053839.

Priestley, C. H. B., and R. J. Taylor, 1972: On the assessment of surface heat flux and evaporation using large-scale parameters. *Mon. Wea. Rev.,* **100,** 81–92.

Reifen, C., and R. Toumi, 2009: Climate projections: Past performance no guarantee of future skill? *Geophys. Res. Lett.,* **36,** L13704, doi:10.1029/2009GL038082.

Roeckner, E., and Coauthors, 2003: The atmospheric general circulation model ECHAM5: Part 1: Model description. Rep. 349, Max-Planck-Institut für Meteorologie, Hamburg, Germany, 127 pp. [Available online at http://www.mpimet.mpg.de/fileadmin/publikationen/Reports/max_scirep_349.pdf.]

Schulla, J., and K. Jasper, 2007: Model Description WaSiM-ETH. Tech. Rep., 181 pp. [Available online at http://wasim.ch/downloads/doku/wasim/wasim_2007_en.pdf.]

Scinocca, J. F., N. A. McFarlane, M. Lazare, J. Li, and D. Plummer, 2008: The CCCma third generation AGCM and its extension into the middle atmosphere. *Atmos. Chem. Phys. Discuss.,* **8,** 7883–7930.

Skamarock, W. C., and Coauthors, 2008: A description of the Advanced Research WRF version 3. NCAR Tech. Note NCAR/TN-475+STR, 113 pp. [Available online at http://www.mmm.ucar.edu/wrf/users/docs/arw_v3.pdf.]

Smiatek, G., H. Kunstmann, R. Knoche, and A. Marx, 2009: Precipitation and temperature statistics in high-resolution regional climate models: Evaluation for the European Alps. *J. Geophys. Res.,* **114,** D19107, doi:10.1029/2008JD011353.

Wagner, S., P. Berg, G. Schädler, and H. Kunstmann, 2013: High resolution regional climate model simulations for Germany: Part II—Projected climate changes. *Climate Dyn.,* **40,** 415–427, doi:10.1007/s00382-012-1510-1.

Wilby, R. L., and I. Harris, 2006: A framework for assessing uncertainties in climate change impacts: Low-flow scenarios for the River Thames, UK. *Water Resour. Res.,* **42,** W02419, doi:10.1029/2005WR004065.

——, L. E. Hay, W. J. Gutowski, R. W. Arritt, E. S. Takle, Z. Pan, G. H. Leavesley, and M. P. Clark, 2000: Hydrological responses to dynamically and statistically downscaled climate model output. *Geophys. Res. Lett.,* **27,** 1199–1202.

Xu, Z., and Z. L. Yang, 2012: An improved dynamical downscaling method with GCM bias corrections and its validation with 30 years of climate simulations. *J. Climate,* **25,** 6271–6286.

Yang, D., S. Ishida, B. E. Goodison, and T. Gunther, 1999: Bias correction of daily precipitation measurements for Greenland. *J. Geophys. Res.,* **104** (D6), 6171–6181.